1

Multi-BD Symbiotic Radio-Aided 6G IoT Network: Energy Consumption Optimization with QoS Constraint Approach

Rahman Saadat Yeganeh [1], Mohammad Javad Omidi [1] and

Mohammad Ghavami [2], *Senior Member, IEEE*

Abstract

Symbiotic radio (SR) is a novel paradigm in cognitive ambient backscatter communication, which connects devices without the need to allocation of the frequency spectrum and complex energy infrastructure. Green communication can be realized in 6G networks using symbiotic radio concept. In this paper, we consider a base station (BS) with the active antennas, symbiotic backscatter devices (SBDs) and symbiotic user equipments (SUE). The main purpose is to minimize the energy consumption (EC) in the SR network and increase energy efficiency (EE), while providing the minimum required throughput for SBDs. To this end, a new scheduling scheme called Timing SR (T-SR) is introduced as optimal resource allocation for SBDs. In this system, SBDs harvest energy from ambient signals and then send their information without interfering with each other to the SUE by using the carrier of ambient signal. The main optimization problem has non-convex objective functions and constraints. To solve it, novel mathematical methods called conic quadratic representation (CQR) and sequential quadratic (SQ) techniques are used. Finally, simulation results demonstrate the superiority of the proposed method compared to other outlined schemes in reducing the EC.

Index Terms

Symbiotic radio, backscatter communication, 6G, energy efficiency, IoT, optimal resource allocation.

[1]Department of Electrical and Computer Engineering, Isfahan University of Technology, Isfahan, IR 8415683111

[2]Electrical and Electronic Engineering Department, London South Bank University, London SE1 0AA, U.K.

I. INTRODUCTION

A. Background

With the exponential increase of the internet-of-things (IoT) and wireless devices in the future wireless networks and the required massive connectivity, EC will increase dramatically. This is a big challenge for future networks [1] and is one of the most crucial requirements for the design and implementation of IoT networks [2], [3]. Generally, cellular and IoT devices are usually powered by batteries or other embedded energy sources [4] and this is contrary to the requirements of the Internet of Everything (IoE) in beyond 5G (B5G) and 6G networks [5]. Also, it is not practical to replace/recharge the batteries regularly, especially in harsh environments like toxic nuclear areas [6], large-scale network systems, and building-embedded applications [7]. To implement the infrastructure of future networks, and achieve sustainable and green IoT, it is essential to build a self-sustaining system to reduce maintenance costs [8]–[10]. The best way to achieve the above goals is to use wireless energy harvesting [11]–[13] to improve the EE of the network significantly [14]–[16].

Wireless energy harvesting benefits from active and passive technologies developed for telecommunication systems and networks, such as wireless powered communication networks (WPCN) [17], simultaneous wireless information and power transfer (SWIPT) [18], reconfigurable intelligent surface (RIS), bistatic and ambient backscatter communication (AmBC) [19] and SR [20]. Moreover, AmBC, cognitive radio (CR) and SR can also be used for spectrum sharing [21].

CR technology has been considered to enhance spectrum efficiency in IoT networks [22]. In this system, the secondary user is allowed to access the spectrum allocated to the primary user in an opportunistic or spectrum sharing manner, which makes it challenging to increase the spectrum efficiency [23], [24]. On the other hand, user equipment in the CR system uses the power consuming active components, which leads to reduced device battery life, and limits the development of emerging services in future wireless networks [25].

In recent years, AmBC has been used to design transceivers without requiring active RF components, thus the power consumption can be greatly reduced. It can make battery-free communications with enhanced EE. Also, AmBC enables backscatter devices (BDs) to modulate their information over the ambient RF signals (such as Cellular, TV, or WiFi signals); therefore, there is no need for complex processes to reallocate frequency (which is very limited) to BDs; hence, spectral efficiency (SE) is greatly enhanced [19], [26].

There are some disadvantages to AmBC since ambient RF sources are dynamic, and thus the performance of an AmBC may not be stable. Also, since the transmission power and position of ambient RF sources are not controllable, the deployment of an AmBC to achieve optimal performance is more complex. On the other hand, AmBC and BS signals may interfere with the receiver as they both send signals at the same operating frequency [27].

In a 6G network, the low EC, extended battery life and increased efficiency of the allocated frequency band are three important research areas [28], [29]. The main purpose of 6G communications is to make the devices battery-free whenever and wherever possible [30].

In this paper, a new technique called symbiotic radio (SR) system with a resource scheduling system called timing-SR or T-SR is proposed to use the benefits and overcome the drawbacks of AmBC and CR as a promising solution to green IoT networks. It can enhance spectrum efficiency by using mutualism sharing the spectrum and also can increase EE by using the semi-passive structure [31]–[34]. In the SR system, SBDs harvest the energy from ambient signals wirelessly, in the cellular or cell-free networks and establish stable communications [35], [36]. Moreover, the transmitter and receiver communicate in a coexistence manner; hence, the SR can support massive wireless connections in dense networks [22], [25];

B. Related Works

Energy efficiency, as an objective, is brought up in many types of research. In [37], authors consider a basic SR model which consists of three nodes BS, BD, and UE. The BS beamform its signal to establish joint primary and BD transmissions, while the UE can decode the signals from both BS and the BD separately.

In [38], authors tried to reach the maximum EE with efficient resource allocation among BDs while maintaining the quality of service (QoS) for users in NOMA-backscatter communication (BC) networks. To overcome the drawbacks of the BC systems, the SR system has been considered in [39]. In this paper, the authors consider the EE maximization problem of SR system with multiple BDs, which enables the harvesting of energy from ambient signal. In the Scheduling system, the time division multiple access (TDMA) protocol is used and BDs take turns to modulate their information on the ambient signal and send their information to the receiver.

The symbiotic communication model with multiple BDs was proposed in [40]. For this purpose, users use mutually coding and decoding algorithms to achieve orthogonal chips with

different chip lengths and chip transmission rates. Hence, the interference-free transmission between multiple user signals is realized, and users can send their information concurrently. Also, in [41], the authors consider a multi-BD SR system in which a cooperative receiver can receive and detect the collected data from the PT and multiple BDs, simultaneously. For this purpose, they assume a random code-assisted multiple access scheme for the multi-BD, with which the transmit power of the BS and the reflection coefficients of the BDs are jointly optimized. In this scheme, each BD chooses its random code to backscatter its information instantaneously.

C. Contribution

The number of IoT devices and data rates for transmitting information in future heterogeneous networks is increasing rapidly [42]. Therefore, there is a need to use new frequency spectrums and also the EC of these networks will increase sharply. As mentioned in the previous section, EE is gradually accepted as an important design criterion for future networks [43], because proper EE has several benefits including reducing greenhouse gas emissions [44], reducing demand for energy imports, and reducing the complex implementation of networks and improved economy [45]. In accordance, we study a novel cognitive backscattering system based on wireless power transfer in a system with low power consumption to enhance EE (which is defined as the ratio between the instantaneous throughput and the total energy consumption) of dense networks such as cellular or cell-free communication and IoT networks. In this paper, we use SR system technology to prevent interference between IoT devices and ambient transmitters, as well as to eliminate the need for IoT devices to reallocate spectrum and use ambient energy signals to extend their life. In our system model, we try to minimize the network EC by guaranteeing a minimum required throughput for multiple IoT devices (SBDs) that were randomly distributed in the network.

The major contributions of this paper are summarized as follows:

- First, we present a general system model for the proposed SR system and investigate that when SBDs have information to send, they can send it to their intended destination. In this model, a QoS constraint is considered to guarantee the minimum transmission rate of SBDs.

- For the SBDs in the SR network the T-SR mode has been introduced for timing resource allocation. In the T-SR model we consider 2-modes variable time slot consisting of energy harvesting and environment sensing (EHS) and modulation and transmission of information

(MTI) modes. In these strategies, users can always harvest energy as much as needed to transmit their information which helps to reduce EC in the network because SBDs do not have idle mode. Also, they can send their information in continuous time slots without interfering with other SBDs.

- The general proposed model is formulated by a non-convex optimization problem with an objective function to minimize EC in the network subject to the required SBDs throughput and amount of energy harvesting. The non-convex optimization problem is reformulated and solved by two novel mathematical techniques referred to sequential quadratic (SQ) and conic quadratic representation (CQR).

- The EC in the proposed SR system with the T-SR scheduling mode is compared with the TDMA mode. Also, we show that the SR system is suitable for dense networks such as IoT and 6G networks and it is compared with other well-known IoT protocols.

The remainder of this paper is organized as follows. Section II introduces the proposed system model for the SR. In Section III, we investigate the EC problem by considering the minimum user throughput requirement. Moreover, in this section SQ and CQR methods are introduced and the main problem is solved by using them. In Section IV, the computational complexity of the proposed methods is analyzed. In section V, to confirm our analytical findings, the results of the simulations and comparisons with other work are performed, finally, the conclusions and future work are given in section VI.

Notations: $\langle a, b \rangle$ denotes the inner product of a and b, $Tr\left(\mathbf{A}\right)$, $\mathbf{A}^H$, $\mathbf{A}^T$, $\|\mathbf{A}\|$ denote the trace, conjugate transpose, transpose, and norm of the matrix $\mathbf{A}$, respectively. The positive semi-definite was denoted as $\mathbf{A} \succeq 0$ and ∇ shows the gradient operator.

II. SYSTEM MODEL

As illustrated in the system model of Fig.1, in the symbiotic radio (SR) system, the base stations (BS) equipped with N array antennas, one symbiotic user equipment (SUE) with a single antenna and I single antenna symbiotic backscatter devices (SBDs) are considered. The SBDs are randomly distributed and harvest energy from the ambient signal transmitted by BS. In the proposed SR system, we consider two main operating phases. In the first phase, SBDs receive a signal from BS, and harvest as much energy as needed from the received signal. In this phase, SBDs, as IoT devices, can constantly sense the environment using embedded sensors
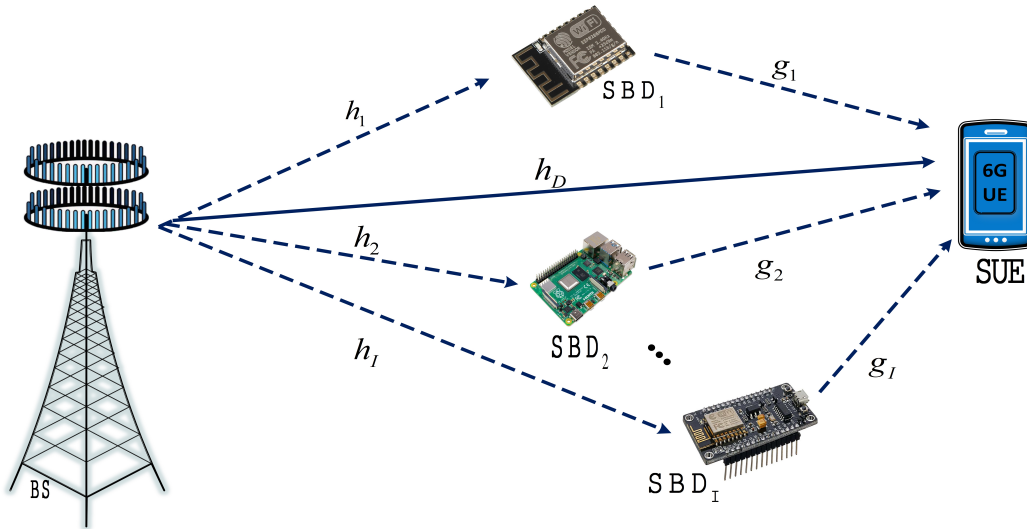
Fig. 1: Symbiotic radio system model with multiple SBDs

(such as temperature, humidity, pressure, etc.); hence, this phase is called energy harvesting and environment sensing (EHS). In the second phase, SBDs modulate their information on the received BS signal and send their data to SUE. Therefore, this phase is called modulation and transmission of information (MTI) by SBDs. In all situations, it is assumed that channel state information (CSI) is fully available.

SBDs can use the RF frequency of the received ambient signal from the nearest BSs. In this case, based on the frequency division multiple access (FDMA) method, and due to the coexistence of devices in the SR networks, the separation of SBDs information is well carried out in SUE [46]. Otherwise, if several SBDs are covered by one BS (Similar to Fig.1), they may use the same carrier frequency to modulate and send their information simultaneously. In this worst case situation, SBDs and SUE should use mutually coding and decoding algorithms to achieve orthogonal chips with different chip lengths and chip transmission rates. Hence, the interference-free transmission between multiple user signals is realized, thereby achieving multi-user symbiosis [40], [41]. Also, in the SR system, since SUE and SBDs exchange information in a collaborative manner, and the SUE has information about the signal characteristics sent by the SBDs, it can separate the information of SBDs correctly, and thus, interference of the SBDs information is reduced in SUE and can be ignored [25], [47].

The SBDs receive the ambient signal from BS in $\tau_j, j = 1, 2, ..., J$ time slots. In this timing system, J is the total number of time slots allocated to SBDs on the network, which is assumed
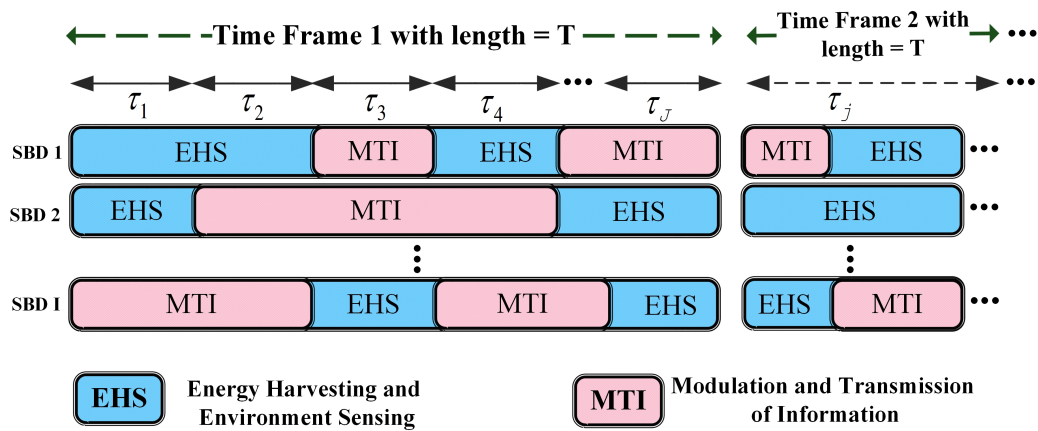
Fig. 2: The TDD frame for EHS and MTI modes in T-SR instantaneous transmission model

to be equal to I. In the SR system, the time slots are identical and SBDs are allowed to use one or more time slots in each frame. The number of time slots required to send information is proportional to the length of information in each SBD and the energy required to send this information. In Fig.2, the scheduling of energy harvesting by SBDs and data transmission from SBDs to SUEs is shown. In the SR system, we define this time division duplexing (TDD) as timing-SR (T-SR) mode. In each time frame with the length of T, SBDs start data transmission at the beginning of a time slot and finish at the end of that or another time slot. We define υ as the set of all time slots used for data transmission. For example, in Fig.2 the data is transmitted by SBD_2 in τ_2, τ_3 and τ_4 time slots so $\upsilon = \{2, 3, 4\}$. Therefore, in T-SR model:

$$\tau_{j=1,2,\ldots,J} = \begin{cases} \mathrm{MTI} & j \in \upsilon \\ \mathrm{EHS} & j \notin \upsilon \end{cases} \tag{1}$$

It is assumed that all SBDs have the required initial charges. With a single antenna, SBDs can only either harvest energy or transmit signal at a time. Hence, during the transmission, SBDs will switch from MTI mode to EHS whenever they need to recharge the battery.

The T-SR mode in the SR network is used to increase EE and throughput. Moreover, there is no need to perform complex processing on the network core to reallocate frequency to SBD devices, as they use ambient signal frequencies. In this paper, we will study the EC of the SR system and will compare EC in the SR scheduling method (T-SR) with the TDMA scheme in the simulation section.

A. Problem Formulation

In Fig.1, we assume that the BS with N antennas and SBDs and SUE are single antenna. The signal transmitted by n-th antenna on BS to all SBDs in j-th time slot is denoted by $x_{n,j}$ with zero mean and $\mathrm{E}\left[|x_{n,j}|^2\right] = p_{BS}$ which is the transmit power of n-th antenna. In this paper, p_{BS} is considered in $x_{n,j}$ and it is not shown in relations. The signal vector at the time slot τ_j is defined as $\mathbf{x}_j \triangleq [x_{1,j}, x_{2,j}, ..., x_{N,j}]^T$ and the channel vector from n-th antenna to SBD$_\mathrm{i}$ is modeled by $h_{n,i}$. Hence, the complex channel vector to SBD$_\mathrm{i}$ is $\mathbf{h}_i \triangleq [h_{1,i}, h_{2,i}, ..., h_{N,i}]^T$ which is flat fading and constant during a one time frame. Therefore, the received signal in the SBD$_\mathrm{i}$ at the time slot τ_j is:

$$y_{i,j} = \mathbf{h}_i^H \mathbf{x}_j + n_i \ , \quad i, j \in \boldsymbol{\Psi} \tag{2}$$

where $\boldsymbol{\Psi} \triangleq [1, 2, ..., I]$ and $n_i \sim CN(0, \sigma_i{}^2)$ is the circularly symmetric complex Gaussian (CSCG) noise and it is assumed to be independent of the signal $\mathbf{x}_j$. According to Eq.(2), the maximum energy harvested by the SBD$_\mathrm{i}$ in the $\tau_{j \notin v}$ is:

$$\varepsilon_{ij} = \eta_i \tau_{j \notin v} \mathbb{E}\left[|y_{i,j}|^2\right] \approx \eta_i \tau_{j \notin v} \mathbf{x}_j^H \mathbf{h}_i \mathbf{h}_i^H \mathbf{x}_j \ , \quad i, j \in \boldsymbol{\Psi} \tag{3}$$

where $0 \leq \eta_i \leq 1$ is the efficiency of energy harvesting or reflection coefficient by SBD$_\mathrm{i}$.

The total energy sent by BS is the sum of energy sent by each of antennas ($\mathrm{E_T}$), so:

$$\mathrm{E_T} = \sum_{n=1}^{N} E_{T_{BS}}^n \tag{4}$$

$\mathrm{E_T}$ can also be expressed as the sum of the energy of transmitted signals by BS at all times during a frame.

$$\mathrm{E_T} = \sum_{j=1}^{J} \tau_j \mathbf{x}_j^H \mathbf{x}_j \ , \quad j \in \boldsymbol{\Psi} \tag{5}$$

The main purpose of this paper is to minimize $\mathrm{E_T}$ to increase EE in the SR system while satisfying the minimum required data rate of the SBDs. In the SR networks, IoT devices with special electronic circuits with very low power consumption close to a passive device are used; therefore, it can be considered that all power consumptions other than radiation power (such as circuit power consumption, etc.) is ignored in our model. In a real-world urban environment, SBDs may be covered by multiple BSs and can harvest energy from all ambient signals, this is faster than harvesting energy from one broadcasting antenna.

The signal $\mathbf{h}_i^H \mathbf{x}_j s_i$, is sent by the SBD$_i$. Where $\mathbf{s_i} \triangleq [s_{i,a}, s_{i,b}, ..., s_{i,z}]_{\{a,b,...,z\}\in \upsilon}^T$ is the normalized modulated information signal transmitted from SBD$_i$ to the SUE in all time slots of the MTI set (υ). Therefore, the received signal at SUE, transmitted by BS and SBD$_i$ in the time slot $\tau_{j\in \upsilon}$ is:

$$y_{i,j\in \upsilon}^{UE} = \sqrt{p_i}\eta_i \mathbf{h}_i^H \mathbf{x}_j g_i s_{i,j\in \upsilon} + \sqrt{p_i}\eta_i g_i s_{i,j\in \upsilon} n_i + \mathbf{h}_D^H \mathbf{x}_j + n_{UE} \tag{6}$$

Where g_i is the complex channel gain from SBD$_i$ to SUE and p_i is the backscattered power of SBD$_i$ to transmit the signals and $n_{UE} \sim CN(0, \sigma_{UE}{}^2)$ is the CSCG noise at the SUE. Note that since SBDs have a passive antenna, they receive little noise. Also, the power of the second term of Eq.(6) is much smaller than of the n_{UE} due to the pathloss link. So, the noise of SBDs can be negligible when backscattering data [41], [48]. The third term of $y_{i,j\in \upsilon}^{UE}$, which is the signal sent from the BS through the direct link to the SUE, is an interference to the desired signal sent by the SBDs. Since this signal has a higher power than the SBDs signal, it can be removed by various techniques such as successive interference-cancellation (SIC) [26], [49], [50]. According to the above description and assuming the beamforming vector of active array antenna on BS be equal to 1, the SNR for decoding $s_{i,j\in \upsilon}$ in the SUE is:

$$SNR_i^{UE} = \frac{p_i \left| \eta_i g_i \sum_{n=1}^N h_{n,i} \right|^2}{\sigma_{UE}^2} \tag{7}$$

Since in the SR network, the semi-passive IoT devices are used, and These devices do not have active RF components that consume a lot of power; therefore, it can be considered that each SBD uses almost all amount of harvested energy to send their signals, then the relation $p_i \tau_{j\in \upsilon} \approx \sum_{j=1,j\notin \upsilon}^J \varepsilon_{ij}$ is established and Eq.(7) can be rewritten as follows ($\sum_{n=1}^N h_{n,i} \triangleq h_{Ti}$):

$$SNR_i^{UE} = \frac{|g_i \eta_i h_{Ti}|^2 \sum_{j=1,j\notin \upsilon}^J \varepsilon_{ij}}{\tau_{j\in \upsilon}\sigma_{UE}^2} \tag{8}$$

III. ENERGY AND RATE OPTIMIZATION

In this section, an optimization problem is proposed. We aim to minimize the sum of the transmit energy by all BS by jointly optimizing the transmit energy and information signal, time scheduling, and energy harvesting by SBDs. Also, the energy of the signal transmitted by BS must satisfy the minimum specified SBDs information rate, defined as C_i. To ensure that each of the SBDs can send its information to the destination (SUE) in the minimum throughput C_i,

we use the Shannon channel capacity relation to specify the minimum capacity for the channel between them and consider the constraint for all SBDs. Therefore, the instantaneous achievable rate per unit bandwidth (SE) (bps/Hz) of the SBD_i with considering the normalized bandwidth of the channel to 1Hz, is:

$$R_i = \tau_{j \in \upsilon} \log_2 \left(1 + SNR_i^{UE}\right) \geq C_i \tag{9}$$

According to the above description and Eq.(3) and Eq.(9), the general optimization problem for the mentioned objectives and constraints is defined as follows:

$$\min_{\mathbf{x}_j, \tau_j, \varepsilon_{ij}} \quad \mathrm{E_T} = \sum_{j=1}^{J} \tau_j \mathbf{x}_j^H \mathbf{x}_j \tag{10}$$

$$\text{s.t.} \quad R_i \geq C_i \qquad\qquad i \in \boldsymbol{\Psi} \tag{10a}$$

$$\tau_j \geq 0 \qquad\qquad j \in \boldsymbol{\Psi} \tag{10b}$$

$$\sum_{j=1}^{J} \tau_j \leq T \qquad\qquad j \in \boldsymbol{\Psi} \tag{10c}$$

$$\varepsilon_{ij} \leq \eta_i \tau_{j \notin \upsilon} \mathbf{x}_j^H \mathbf{h}_i \mathbf{h}_i^H \mathbf{x}_j \qquad i, j \in \boldsymbol{\Psi} \tag{10d}$$

The problem of Eq.(10) is non-convex due to objective function and constraint (10d). However, constraint (a) is convex since it can be seen as a composition of perspective of $\log\left(1 + \alpha x\right), a > 0$ and an affine function of $x = \varepsilon_{ij}$. To overcome the non-convexity of objective function, an auxiliary variable $\gamma_j = \mathbf{x}_j^H \mathbf{x}_j$ is defined and as a result, another non-convex constraint appears. It can be relaxed by adding the following convex constraint:

$$\gamma_j \geq \mathbf{x}_j^H \mathbf{x}_j \quad, j \in \boldsymbol{\Psi} \tag{11}$$

So, the new problem is:

$$\min_{\mathbf{x}_j, \tau_j, \gamma_j, \varepsilon_{ij}} \quad \mathrm{E_T} = \sum_{j=1}^{J} \tau_j \gamma_j \tag{12}$$

$$\text{s.t} \quad (10a), (10b), (10c), (10d) \tag{12a}$$

$$\gamma_j \geq \mathbf{x}_j^H \mathbf{x}_j \qquad j \in \boldsymbol{\Psi} \tag{12b}$$

The problem (12) is still non-convex. Also, this problem contains the perspective of logarithm function which is convex but not disciplined convex. Disciplined convex problems can be solved efficiently by using the primal-dual interior point method and solver technologies progressed

maturely over recent years. In the four following subsections (A, B, C, D), the non-convexity parts of the general optimization problem are investigated, and the problem will become convex by various techniques.

A. Overcoming Non-Convex Objective Function

To overcome the non-convexity of objective function we can rewrite it as follows:

$$\sum_{j=1}^{J} \tau_j \gamma_j = \frac{1}{4} \left[\sum_{j=1}^{J} \left(\tau_j + \gamma_j \right)^2 - \sum_{j=1}^{J} \left(\tau_j - \gamma_j \right)^2 \right], j \in \boldsymbol{\Psi} \tag{13}$$

Eq.(13) is the difference between two convex functions. By definition $f_1 \triangleq \left(\tau_j - \gamma_j \right)^2$, the second term $-f_1$ is a concave function and its upper bound can be calculated by a linear function. The upper bound of that relation performed by inner approximation [51] and sub-gradient method [52] around the feasible (initial) point $\left(\hat{\tau}_j, \hat{\gamma}_j \right)$ as follows:

$$\begin{aligned} f_1 &\leq \left(\hat{\tau}_j - \hat{\gamma}_j \right)^2 + \nabla_{\tau_j, \gamma_j} f_1 \left(\hat{\tau}_j, \hat{\gamma}_j \right) \left[\left(\tau_j - \hat{\tau}_j \right), \left(\gamma_j - \hat{\gamma}_j \right) \right]^T \\ &= \left(\hat{\tau}_j - \hat{\gamma}_j \right)^2 + 2 \left(\hat{\tau}_j - \hat{\gamma}_j \right) \left[\left(\tau_j - \hat{\tau}_j \right) - \left(\gamma_j - \hat{\gamma}_j \right) \right] \end{aligned} \tag{14}$$

Eq.(14) is replaced in the second part of Eq.(13) and in results an upper-bounded function which is a tangent line to the original function. It is shown in [51], that the upper-bounded approximation function lies quite close to the function, at least near the point of tangency which is the point placed on Eq.(13). Suppose Eq.(14) is iteratively solved and converged. Therefore, the relations (13) and (14) attain the same local optimal point.

B. Semidefinite Relaxation of Constraint (10d)

By using the trace commutative property, we have the following equation:

$$\mathbf{x}_j^H \mathbf{h}_i \mathbf{h}_i^H \mathbf{x}_j = \mathrm{Tr} \left(\mathbf{x}_j^H \mathbf{h}_i \mathbf{h}_i^H \mathbf{x}_j \right) = \mathrm{Tr} \left(\mathbf{x}_j \mathbf{x}_j^H \mathbf{h}_i \mathbf{h}_i^H \right) \tag{15}$$

Now the constraint $(10d)$ can be reformulated by an auxiliary matrix $\mathbf{X}_j = \mathbf{x}_j \mathbf{x}_j^H$ and $\mathbf{H}_i \triangleq \mathbf{h}_i \mathbf{h}_i^H$ as follows:

$$\varepsilon_{ij} \leq \eta_i \tau_{j \notin v} Tr \left(\mathbf{X}_j \mathbf{H}_i \right) \qquad i, j \in \boldsymbol{\Psi} \tag{16}$$

So, since $\mathbf{X}_j$ is a positive semidefinite matrix, the constraint (16) can be replaced by:

$$\eta_i \tau_{j \notin v} Tr \left(\mathbf{X}_j \mathbf{H}_i \right) / \varepsilon_{ij} \geq 1 \qquad i, j \in \boldsymbol{\Psi} \tag{17a}$$

$$\mathbf{X}_j \succeq 0 \qquad j \in \boldsymbol{\Psi} \tag{17b}$$

$$\mathrm{Rank} \left(\mathbf{X}_j \right) = 1 \qquad j \in \boldsymbol{\Psi} \tag{17c}$$

where the notation $\succeq$ denotes that $\mathbf{X}_j$ is a positive semidefinite. The problem is still non-convex due to the rank-one constraint given in $(17c)$. By applying the semidefinite relaxation (SDR) technique, the rank-one constraint will be dropped, and the relaxed version of the main problem will be obtained [53]. The relaxed problem will be a convex semidefinite programming (SDP) problem that is solvable by interior-point methods. If the optimal solution $\mathbf{X}_j$ for the problem with the relaxed constraints (17) is rank-one, then it is also a solution for the original problem (12), which can be done by using randomization techniques [53]. In this state, we can easily extract a feasible $\mathbf{x}_j$ from $\mathbf{X}_j$.

Moreover, we know $\mathrm{Tr}(\mathbf{X}_j) \leq \lambda_{\max}(\mathbf{X}_j)$, where $f_2 \overset{\Delta}{=} \lambda_{\max}(\mathbf{X}_j)$ denotes the maximum eigenvalue of the $\mathbf{X}_j$ and it can be rewritten as the following difference between two convex functions [54]:

$$\mathrm{Tr}\left(\mathbf{X}_j\right) - \lambda_{\max}\left(\mathbf{X}_j\right) \leq 0 \tag{18}$$

The sub-gradient of $\lambda_{\max}(\mathbf{X}_j)$ is:

$$\nabla_{\mathbf{X}_j} f_2\left(\hat{\mathbf{X}}_j\right) = \mathbf{v}_{\max}\left(\mathbf{X}_j\right)\mathbf{v}_{\max}^H\left(\mathbf{X}_j\right) \tag{19}$$

where $\mathbf{v}_{\max}\left(\mathbf{X}_j\right)$ is the maximum eigenvector corresponding to the $\lambda_{\max}(\mathbf{X}_j)$. Therefore, the lower bound of linear approximation $\lambda_{\max}(\mathbf{X}_j)$ at the point $\hat{\mathbf{X}}_j$ is as follows:

$$\begin{aligned} f_2 &\geq \lambda_{\max}\left(\hat{\mathbf{X}}_j\right) + \left\langle \nabla_{\mathbf{X}_j} f_2\left(\hat{\mathbf{X}}_j\right), \left(\mathbf{X}_j - \hat{\mathbf{X}}_j\right)\right\rangle \\ &= \lambda_{\max}\left(\hat{\mathbf{X}}_j\right) + \mathbf{v}_{\max}^H\left(\hat{\mathbf{X}}_j\right)\mathbf{v}_{\max}\left(\hat{\mathbf{X}}_j\right)\left(\mathbf{X}_j - \hat{\mathbf{X}}_j\right) \end{aligned} \tag{20}$$

By substituting Eq.(20) in the Eq.(18) the following relationship is obtained:

$$\mathrm{Tr}\left(\mathbf{X}_j\right) \leq \mathbf{v}_{\max}^H\left(\hat{\mathbf{X}}_j\right)\mathbf{X}_j\mathbf{v}_{\max}\left(\hat{\mathbf{X}}_j\right) \tag{21}$$

Eq.(21) is defined as a convex subset of the convex set of the original equation (12) and is moved to the objective function with multiplying in coefficient ℓ as a penalty function [55]. The resulting problem should be solved iteratively for ℓ from small to large values, so as not to cause numerical instability. Herein, the constraint $(17a)$ can be represented by the difference in the convex functions method and by defining the auxiliary variable $\phi_{ij}^2 = \varepsilon_{ij}$:

$$\phi_{ij}^2 \leq \eta_i \tau_{j \notin \upsilon} Tr\left(\mathbf{X}_j \mathbf{H}_i\right) \tag{22}$$

The above inequality is equivalent to:

$$\phi_{ij}^2 + \frac{1}{4}(\eta_i Tr\left(\mathbf{X}_j \mathbf{H}_i\right) - \tau_{j \notin \upsilon})^2 \leq \frac{1}{4}(\eta_i Tr\left(\mathbf{X}_j \mathbf{H}_i\right) + \tau_{j \notin \upsilon})^2 \tag{23}$$

Since $Tr\left(\mathbf{X}_j\mathbf{H}_i\right) + \tau_{j\notin v} \geq 0$, the above CQR relation can be written in the following form:

$$\left\|\phi_{ij}, \frac{1}{2}\left(\eta_i Tr\left(\mathbf{X}_j\mathbf{H}_i\right) - \tau_{j\notin v}\right)\right\|_2 \leq \frac{1}{2}\left(\eta_i Tr\left(\mathbf{X}_j\mathbf{H}_i\right) + \tau_{j\notin v}\right) \tag{24}$$

Also, the constraint Eq.(12a) can be written as follows:

$$\gamma_j \geq Tr\left(\mathbf{X}_j\right) \tag{25}$$

By changing the variable $\phi_{ij}^2 = \varepsilon_{ij}$, the constraint $(10a)$ will be non-convex versus the variables $\left(\phi_{ij}, \tau_i\right)$ as it is not a perspective of function $\log\left(1+x\right)$ anymore. In addition, any optimization problem that includes a $\log$ function, will turn the problem into a not disciplined convex problem and cannot be efficiently solved using modern semi-definite programming (SDP) solvers, such as SeDuMi [56]. To overcome this problem, new solutions called sequential quadratic (SQ) and conic quadratic representation (CQR) methods are proposed that will be described in subsections C and D.

C. Sequential Quadratic (SQ)

An auxiliary θ_i variable is defined to convert the constraint $a)$ of Eq.(10) to the two following inequalities:

$$a_1)\ \theta_i \leq \frac{|g_i\eta_i h_{Ti}|^2}{\sigma_{UE}^2}\sum_{j=1,j\notin v}^{J}\phi_{ij}^2 \qquad i, j \in \boldsymbol{\Psi} \tag{26}$$

$$a_2)\ C_i - \tau_{j\in v}\log_2\left(1 + \frac{\theta_i}{\tau_{j\in v}}\right) \leq 0 \qquad i \in \boldsymbol{\Psi} \tag{27}$$

The relation $a_1)$ is not convex and should be using the difference between the convex functions method and linearization of the second part by the first-order approximation. As mentioned in the previous sections, replacing the linear approximation around the initial point, in the second part of Eq.(26):

$$\hat{a}_1)\ \theta_i - \frac{|g_i\eta_i h_{Ti}|^2}{\sigma_{UE}^2}\left(\sum_{j=1,j\notin v}^{J}\hat{\phi}_{ij}^2 + 2\left(\phi_{ij} - \hat{\phi}_{ij}\right)\sum_{j=1,j\notin v}^{J}\hat{\phi}_{ij}\right) \leq 0 \tag{28}$$

Also, the constraint $a_2)$ is convex; however, it is not disciplined due to the logarithm function. One approach for turning it into a disciplined form is to find an upper bound approximation by quadratic form and apply the inner approximation. The following theorem gives an iterative approach similar to inner approximation which converges to the local optimum for a smooth optimization problem.

Theorem: the function $f_3 : D \rightarrow \mathbb{R}, \forall x, \hat{x} \in D$, is convex if a second derivative exists at each point in domain D and $\nabla^2 f_3(\hat{x}) \geq 0$, hence, the second-order approximation is [57]:

$$f_3(x) = f_3(\hat{x}) + \nabla f_3(\hat{x})(x - \hat{x})^T + (x - \hat{x})\nabla^2 f_3(\hat{x})(x - \hat{x})^T \tag{29}$$

According to the above relation, the matrix $\mathbf{H_s}$ (called an upper bound Hessian matrix) must satisfy the following relation:

$$\nabla^2 f_3(\hat{x}) \preceq \mathbf{H_s} \tag{30}$$

If the above relation is established, Eq.(29) can be converted as follows:

$$f_3(x) \leq f_3(\hat{x}) + \nabla f_3(\hat{x})(x - \hat{x})^T + (x - \hat{x})\mathbf{H_s}(x - \hat{x})^T \tag{31}$$

where the function f_3 is defined as the left-hand side of the constraint a_2). The value of $\nabla^2 f_3(\hat{x})$ can be obtained as follows:

$$\nabla^2 f_3(\theta_i, \tau_{j\in v}) = \begin{bmatrix} \frac{\tau_{j\in v}}{(\tau_{j\in v}+\theta_i)^2} & -\frac{\theta_i}{(\tau_{j\in v}+\theta_i)^2} \\ -\frac{\theta_i}{(\tau_{j\in v}+\theta_i)^2} & \frac{\theta_i^2}{\tau_{j\in v}(\tau_{j\in v}+\theta_i)^2} \end{bmatrix} \tag{32}$$

Matrix $\nabla^2 f_3(\theta_i, \tau_{j\in v})$ for $\tau_{j\in v}, \theta_i \geq 0$ does not have an upper bound. Therefore, we consider the below feasible set to bound it (β is a fixed number):

$$D_i = \left\{ (\theta_i, \tau_{j\in v}) | \theta_i \geq 0, 0 \leq \frac{\hat{\tau}_{j\in v}}{\beta} \leq \tau_{j\in v} \leq \infty \right\} \tag{33}$$

This new domain, which is an implicit constraint, is added to the constraints of the main problem. Now to estimate an upper bound of Eq.(32), the following matrix is replaced instead of it (see the proof of this, in the appendix):

$$\nabla^2 f_3(\theta_i, \tau_{j\in v}) \leq \begin{bmatrix} \frac{9\beta}{8\hat{\tau}_{j\in v}} & -\frac{\beta}{8\hat{\tau}_{j\in v}} \\ -\frac{\beta}{8\hat{\tau}_{j\in v}} & \frac{9\beta}{8\hat{\tau}_{j\in v}} \end{bmatrix} \leq \mathbf{H_s} \tag{34}$$

Also, the gradient of Eq.(27) is as follows:

$$\nabla f_3(\theta_i, \tau_{j\in v}) = \begin{bmatrix} -\frac{\tau_{j\in v}}{\tau_{j\in v}+\theta_i}, & -\log\left(1 + \frac{\theta_i}{\tau_{j\in v}}\right) + \frac{\theta_i}{\tau_{j\in v}+\theta_i} \end{bmatrix} \tag{35}$$

Therefore, according to Eqs.(29),(34) and (35), the a_2) constraint is converted to:

$$\hat{a}_2) \, C_i - \hat{\tau}_{j\in v}\log_2\left(1 + \frac{\hat{\theta}_i}{\hat{\tau}_{j\in v}}\right) + \nabla f_3\left(\hat{\theta}_i, \hat{\tau}_{j\in v}\right)\left[\theta_i - \hat{\theta}_i, \tau_{j\in v} - \hat{\tau}_{j\in v}\right]^T$$
$$+ \left[\theta_i - \hat{\theta}_i, \tau_{j\in v} - \hat{\tau}_{j\in v}\right]\mathbf{H_s}\left[\theta_i - \hat{\theta}_i, \tau_{j\in v} - \hat{\tau}_{j\in v}\right]^T \leq 0 \tag{36}$$

Finally, according to Eqs.(10), (12), (13), (14), (17), (21), (24), (25), (28), (33) and (36), the final convex optimization for the SQ approach is obtained as follows:

$$\min_{\substack{\tau_j, \mathbf{X}_j, \gamma_j \\ \phi_{ij}, \theta_i}} E_T = \sum_{j=1}^{J} \left(\begin{array}{c} \frac{1}{4}\left(\tau_j + \gamma_j\right)^2 - \frac{1}{4}\left(\hat{\tau}_j - \hat{\gamma}_j\right)^2 - \frac{1}{2}\left(\hat{\tau}_j - \hat{\gamma}_j\right)\left(\left(\tau_j - \gamma_j\right) - \left(\hat{\tau}_j - \hat{\gamma}_j\right)\right) + \\ \ell\left(Tr\left(\mathbf{X}_j\right) - \mathbf{v}_{\max}^H\left(\hat{\mathbf{X}}_j\right)\mathbf{X}_j\mathbf{v}_{\max}\left(\hat{\mathbf{X}}_j\right)\right) \end{array} \right)$$

$$\text{s.t.} \quad (10b), (10c), (17b), (24), (25), (28), (33), (36)$$

$$(37)$$

Now this problem is discipline and convex. So, the optimal value of variables and objective function for the SQ approach is obtained by the algorithm 1.

Algorithm 1 Sequential Quadratic (SQ)

1- Initialize $\hat{\mathbf{X}}_j, \hat{\phi}_{ij}, \hat{\tau}_j, \hat{\gamma}_j, \hat{\theta}_i, \beta, a$ in the feasible set

2- Choose $\varepsilon \geq 0, \eta \geq 0$

3- **While** $counter < counter_{\max}$

4-   Solve (37) to obtain the solution variables $\mathbf{X}_j, \phi_{ij}, \tau_j, \gamma_j, \theta_i$

5-   **IF** $\left\{ \left\|\mathbf{X}_j - \hat{\mathbf{X}}_j\right\|, \left\|\phi_{ij} - \hat{\phi}_{ij}\right\|, \left\|\tau_j - \hat{\tau}_j\right\|, \left\|\gamma_j - \hat{\gamma}_j\right\|, \left\|\theta_i - \hat{\theta}_i\right\| \right\} > \varepsilon$

6- $\mathbf{X}_j \to \hat{\mathbf{X}}_j, \phi_{ij} \to \hat{\phi}_{ij}, \tau_j \to \hat{\tau}, \gamma_j \to \hat{\gamma}_j, \theta_i \to \hat{\theta}_i$

7-   Go to step 3

8-   **Else**

9-   Check the the Rank one constraint Eq.(18) to be satisfied by $\frac{Tr(\mathbf{X}_j) - \lambda_{\max}(\mathbf{X}_j)}{Tr(\mathbf{X}_j)} \leq \varepsilon$

10- $counter \to counter + 1$

11-   **IF** the constraint is not satisfied in Step 9

12-   then set $\alpha\ell \to \ell$ and go to Step 3

13-   **Else**

14- $(\mathbf{X}_{opt}, \phi_{opt}, \tau_{opt}, \gamma_{opt}, \theta_{opt}) = (\mathbf{X}_j, \phi_{ij}, \tau_j, \gamma_j, \theta_i)$

15-   **End IF**

16- **End IF**

17- **End While**

D. Conic Quadratic Representation (CQR)

An auxiliary variable z_i is introduced to convert the constraint $a)$ to the two following inequalities:

$$a_1)z_i \geq \frac{C_i}{\tau_{j\in v}} \quad , i \in \boldsymbol{\Psi} \tag{38}$$

$$a_2)\log_2\left(1 + \frac{|g_i\eta_ih_{Ti}|^2}{\tau_{j\in v}\sigma_{UE}^2}\sum_{j=1,j\notin v}^{J}\phi_{ij}^2\right) \geq z_i, i \in \boldsymbol{\Psi} \tag{39}$$

To use the above constraints in the main optimization problem, first, we need to ensure that these equations are convex and disciplined. Therefore, some changes should be applied to them (consider $\tau_j, z_i \geq 0, i \in \boldsymbol{\Psi}$):

$$z_i \geq \frac{C_i}{\tau_{j\in v}} \to (z_i + \tau_{j\in v})^2 \geq 4C_i + (z_i - \tau_{j\in v})^2 \tag{40}$$

Since $z_i, \tau_i \geq 0$, the above CQR relation can be written as follows:

$$(z_i + \tau_{j\in v}) \geq \left\|\left[2\sqrt{C_i}, (z_i - \tau_{j\in v})\right]\right\|_2 \tag{41}$$

To simplify the inequality Eq.(39), the new auxiliary variable Ξ_i , $i \in \boldsymbol{\Psi}$ is defined:

$$\Xi_i \leq \frac{|g_i\eta_ih_{Ti}|^2\sum\limits_{j=1,j\notin v}^{J}\phi_{ij}^2}{\tau_{j\in v}\sigma_{UE}^2} \quad , \quad i \in \boldsymbol{\Psi} \tag{42}$$

Therefore

$$1 + \Xi_i \geq e^{z_i}, \ i \in \boldsymbol{\Psi} \tag{43}$$

The constraint of Eq.(43) is non-convex. In general, to solve the above relation, it is needed to approximate it with the following lemma.

Lemma: If a set of auxiliary variables $\zeta_{q,i}, q \in \{1, ..., M+4\}, i \in \boldsymbol{\Psi}$ satisfy the following inequalities, then we can use the CQR method to approximate the equivalent of the $1 + \Xi_i \geq e^{z_i}, \ i \in \boldsymbol{\Psi}$ with is the following linear and conic inequalities.

$$1 + \Xi_i \geq \zeta_{M+4,i}, \qquad\qquad i \in \boldsymbol{\Psi} \qquad (44a)$$

$$1 + \zeta_{1,i} \geq \left\| \begin{bmatrix} 1 - \zeta_{1,i} & 2 + 2^{1-M} z_i \end{bmatrix} \right\|_2, \qquad i \in \boldsymbol{\Psi} \qquad (44b)$$

$$1 + \zeta_{2,i} \geq \left\| \begin{bmatrix} 1 - \zeta_{2,i} & 5/3 + 2^{-M} z_i \end{bmatrix} \right\|_2, \qquad i \in \boldsymbol{\Psi} \qquad (44c)$$

$$1 + \zeta_{3,i} \geq \left\| \begin{bmatrix} 1 - \zeta_{3,i} & 2\zeta_{1,i} \end{bmatrix} \right\|_2, \qquad i \in \boldsymbol{\Psi} \qquad (44d)$$

$$\zeta_{4,i} \geq \zeta_{2,i} + \zeta_{3,i}/24 + 19/72, \qquad i \in \boldsymbol{\Psi} \qquad (44e)$$

$$1 + \zeta_{q,i} \geq \left\| \begin{bmatrix} 1 - \zeta_{q,i} & 2\zeta_{q-1,i} \end{bmatrix} \right\|_2, \qquad q \in \{5, ..., M+4\}, i \in \boldsymbol{\Psi} \qquad (44f)$$

The accuracy of the approximation increases with M, where the suitable value of M is determined in such a way that the problem reaches convergence and has the least complexity at that point. Therefore, M is called the approximation coefficient.

Proof: See [6], [58]

To establish a relation between the variables ϕ_{ij}^2 and Ξ_i the linear approximation for the right-hand side of Eq.(42) should be written similar to previous sections. By placing it in Eq.(42), the new constraint is obtained as follows and should be added to other constraints of the main problem (Eq.(12)):

$$\Xi_i - \frac{|g_i \eta_i h_{Ti}|^2}{\sigma_{UE}^2} \left(\frac{\sum_{j=1, j \notin v}^{J} \hat{\phi}_{ij}^2}{\hat{\tau}_{j \in v}} + \frac{2\phi_{ij} - \hat{\phi}_{ij} \sum_{j=1, j \notin v}^{J} \phi_{ij}}{\hat{\tau}_{j \in v}} - \frac{\tau_{j \in v} - \hat{\tau}_{j \in v} \sum_{j=1, j \notin v}^{J} \phi_{ij}^2}{\hat{\tau}_{j \in v}^2 \sigma_{UE}^2} \right) \leq 0 \qquad (45)$$

Finally, according to Eqs, (10), (12), (13), (14), (17), (21), (24), (25), (41), (44) and (45), the final convex optimization for the CQR approach is obtained as follows:

$$\min_{\substack{\tau_j, \mathbf{X}_j, \gamma_j, z, i \\ \Xi_i, \phi_{ij}, \zeta_{q,i}}} \mathrm{E_T} = \sum_{j=1}^{J} \left(\begin{array}{l} \frac{1}{4}(\tau_j + \gamma_j)^2 - \frac{1}{4}(\hat{\tau}_j - \hat{\gamma}_j)^2 - \frac{1}{2}(\hat{\tau}_j - \hat{\gamma}_j)\left((\tau_j - \gamma_j) - (\hat{\tau}_j - \hat{\gamma}_j)\right) + \\ \ell\left(Tr(\mathbf{X}_j) - \mathbf{v}_{\max}^H(\hat{\mathbf{X}}_j)\mathbf{X}_j \mathbf{v}_{\max}(\hat{\mathbf{X}}_j)\right) \end{array} \right)$$

$$\text{s.t.} \quad (10b), (10c), (17b), (24), (25), (41), (44), (45)$$

$$(46)$$

Now this problem is discipline and convex. So, the optimal value of variables and objective function for the CQR approach is obtained by the algorithm 2.

The advantage of the CQR method is to obtain the optimal solution by increasing the value of the coefficient of approximation (M). At the end of this calculation and after obtaining $\mathbf{X}_j$, the variable $\mathbf{x}_j$ is obtained according to Equation $\mathbf{X}_j = \mathbf{x}_j \mathbf{x}_j^H$.

Algorithm 2 Conic Quadratic Representation (CQR)

1- Initialize $\hat{\mathbf{X}}_j, \hat{\phi}_{ij}, \hat{\tau}_j, \hat{\gamma}_j, \alpha, M$ in the feasible set

2- Choose $\varepsilon \geq 0, \eta \geq 0$

3- **While** $counter < counter_{\max}$

4-   Solve (46) to obtain the solution variables $\mathbf{X}_j, \phi_{ij}, \tau_j, \gamma_j, \Xi_i, \xi_{M+4,i}, z_i$

5- **IF** $\left\{ \left\| \mathbf{X}_j - \hat{\mathbf{X}}_j \right\|, \left\| \phi_{ij} - \hat{\phi}_{ij} \right\|, \left\| \tau_j - \hat{\tau}_j \right\|, \left\| \gamma_j - \hat{\gamma}_j \right\| \right\} > \varepsilon$

6- $\mathbf{X}_j \to \hat{\mathbf{X}}_j, \phi_{ij} \to \hat{\phi}_{ij}, \tau_j \to \hat{\tau}, \gamma_j \to \hat{\gamma}_j$

7-   Go to step 3

8- **Else**

9-   Check the the Rank one constraint Eq.(18) to be satisfied by $\frac{\text{Tr}(\mathbf{X}_j)\text{-}\lambda_{\max}(\mathbf{X}_j)}{\text{Tr}(\mathbf{X}_j)} \leq \varepsilon$

10- $counter \to counter + 1$

11-   **IF** the constraint is not satisfied in Step 9

12-   then set $\alpha\ell \to \ell$ and go to Step 3

13-   **Else**

14- $(\mathbf{X}_{opt}, \phi_{opt}, \tau_{opt}, \gamma_{opt}) = (\mathbf{X}_j, \phi_{ij}, \tau_j, \gamma_j)$

15-   **End IF**

16- **End IF**

17- **End While**

IV. COMPUTATIONAL COMPLEXITY

In this section, the computational complexity are calculated based on the interior-point method [59] for proposed optimization problems. Interior point methods were extended from linear optimization to semi-definite optimization and the polynomial complexity of the algorithm can be obtained theoretically [60]. In this method, the computational complexity of an SDP optimization problem is obtained using the $\mathcal{O}(1)\sqrt{1 + \sum_{i=1}^{I} \kappa_i} \left(n^3 + n^2 \sum_{i=1}^{I} \kappa_i^2 + n \sum_{i=1}^{I} \kappa_i^3 \right) Digits(p, \varepsilon)$. In this relation, the number of accuracy digits in an ε-solution is defined as $Digits(p, \varepsilon) \approx Ln\left(size\left(p\right)/\varepsilon\right)$ where $size(p) = \left((n+1) \sum_{i=1}^{m} \frac{\kappa_i(\kappa_i+1)}{2} \right) + m + n + 3$ is the dimension of the total data of the problem p, and p can be the CQR or SQ problems.

In the complexity relationship, κ is the dimensions of the i-th constraint, n and m is the number of variables and number of constraints of the optimization problem respectively. These

values are calculated and due to the complexity of relationships and for better understanding, the corresponding figure is drawn in the simulation section by using the exact results of the calculations.

V. SIMULATION RESULTS

According to the system model, SBDs are randomly distributed in the network and almost near the SUE. Each IoT device can harvest energy and send its information to the intended SUE, as shown in Fig.1. In all simulations, we consider $T = 10$, $\eta = 0.8$ and $\sigma_i^2 = \sigma_{UE}^2 = -114 \ dBm$. Also, we assume the carrier frequency is 2 GHz, the channel bandwidth is 400 kHz, the pathloss exponents is 3 and the BS antenna gains is equal to 5 dB. All simulation results were obtained by averaging over 1000 randomly generated channels and ten different initialization points in the convex feasible set were considered to ensure the stability of the problems. The distance between BS and SUE is 200 meters and the maximum distance of SBDs from SUE is 100 meters, which are randomly distributed between BS and SUE.

A. Comparison of Proposed Methods

In this paper, two mathematical methods were used to solve the optimization problem called CQR and SQ. In the CQR method, the first step is to obtain the appropriate approximation coefficient; therefore, the diagram of the minimum energy transfer (consumption) by BS versus SBDs throughput requirement in Fig.3 is plotted by assuming approximation coefficients as $M = 1, 2, ..., 6$ in the CQR method. In Fig.3, as expected, with increasing the minimum data transmission rate in SBDs, the total EC in the network transferred by the BS is also increased. As mentioned, the best approximation coefficient must be found for this problem, where the shapes converge to each other. Based on Fig.3, for $M \geq 4$ this event occurs and so the appropriate values are obtained. The optimal value will be obtained by considering the computational complexity according to Fig. 6, and this value is equal to $M = 4$.

Now, two methods that are CQR with $M = 4$ and SQ are compared with each other to see which of these mathematical solutions is more accurate in finding the optimal points. For this case, we change the basic parameters of the network design. One of the important basic parameters is the number of IoT devices in the network; hence, the minimum energy transfer versus SBDs throughput requirement for these two methods is depicted in Fig.4 where the number of SBDs varies from 2 to 4 ($I \in \{2, 3, 4\}$).
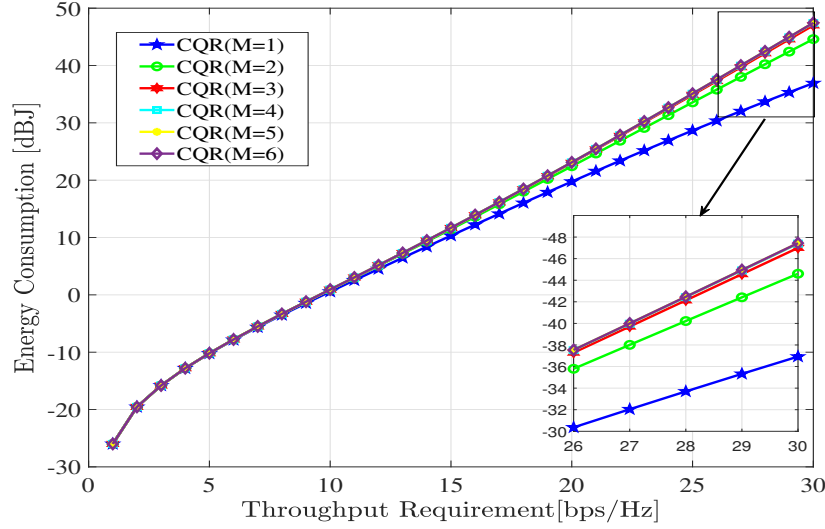
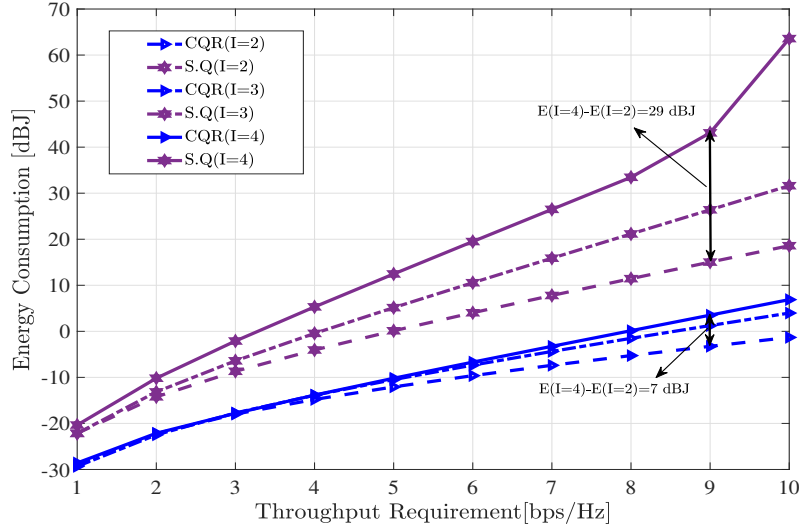Fig. 3: EC versus SBDs throughput requirement in CQR method for $M = 1, 2, ..., 6$, $I = 6$

Fig. 4: EC versus SBDs throughput requirement where the number of SBDs is $I = 2, 3, 4$

In the special case (for example, in $I = 3$), we see that the CQR is the better method to find optimization variables to minimize the total amount of EC in the network by taking into account the fulfillment of the SBDs throughput requirements.

Fig. 5 shows the effect of increasing the number of SBDs in each cell, on the amount of EC in the network, which grows dramatically with the increasing number of SBDs. The EC in two cases of 2 SBDs and 4 SBDs in the SQ method at rate 9 bps/Hz, differs 29dB and in the CQR method this difference equals to 7dB. Therefore, stability and EC in the CQR method are much
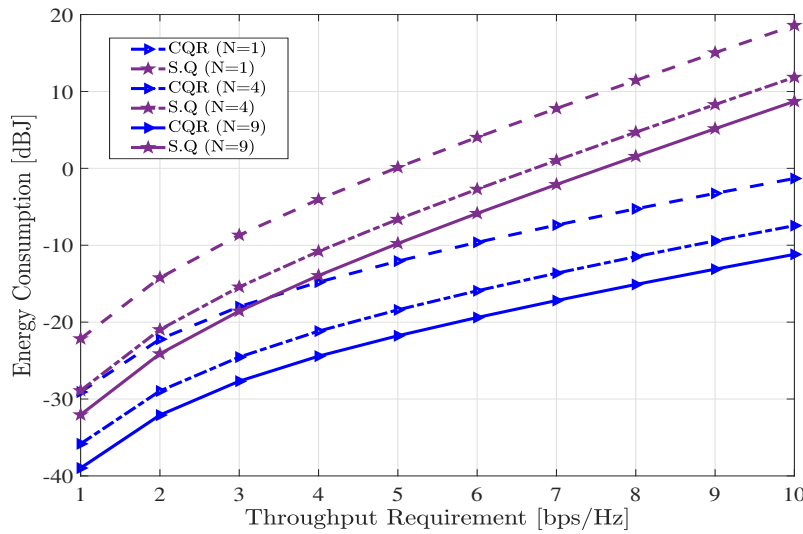
Fig. 5: EC versus SBDs throughput requirement where the number of BS antennas is $N = 1, 4, 9$

better than in the SQ method with increasing the number of SBDs.

Another important parameter is the change in the number of energy output antennas on BS. So, Fig.5 shows this for several antennas in each BS which is a single antenna, 2×2 and 3×3 antennas. It is observed that, with increasing the number of antennas in each BS, the amount of energy consumed in the network is decreased. This is because that, the energy is sent to users with narrower beams with a higher power level and hence, the energy losses will reduce and the SBD batteries charge quickly; therefore, energy waste is significantly reduced.

B. Computational Complexity

The simulation of the computational complexity of the SQ and CQR methods, which is presented in Section IV, is shown in Fig. 6. In this figure, the number of IoT devices (SBDs) is variable. According to Fig.6, The computational complexity of the CQR method is higher than the SQ method in cases where the number of devices in the network is small, and it is lower than the SQ for networks with high user density. Therefore, the proposed main methods can be used well in the IoT networks with a large number of users. Also, in the CQR, with increasing the value of M, The complexity of the algorithm increases slightly.

According to Fig.6 and descriptions of the previous sections, in the CQR method, the appropriate approximation coefficient where there is the least complexity and closest convergence with other values in the function, is $M = 4$.
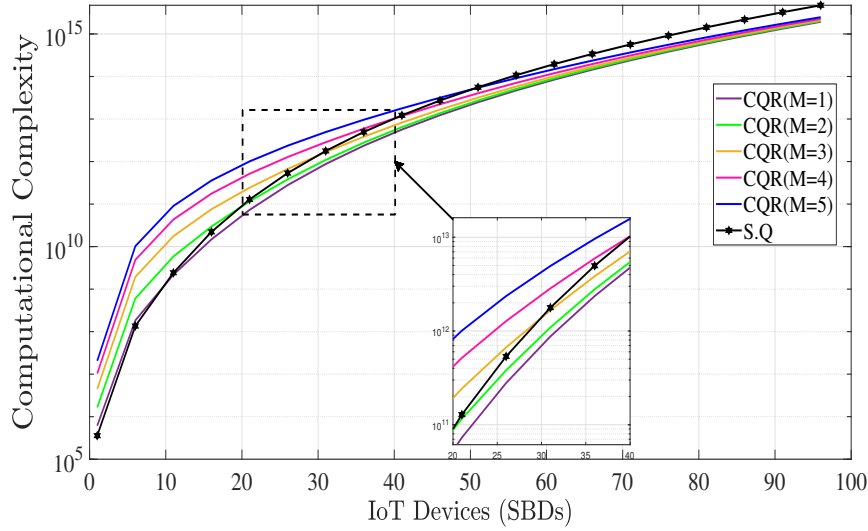
Fig. 6: The computational complexity of investigated methods where the number of SBDs changes from 1 to 100, $N = 4$ and $\varepsilon = 10^{-6}$

EHS — Energy Harvesting and Environment Sensing
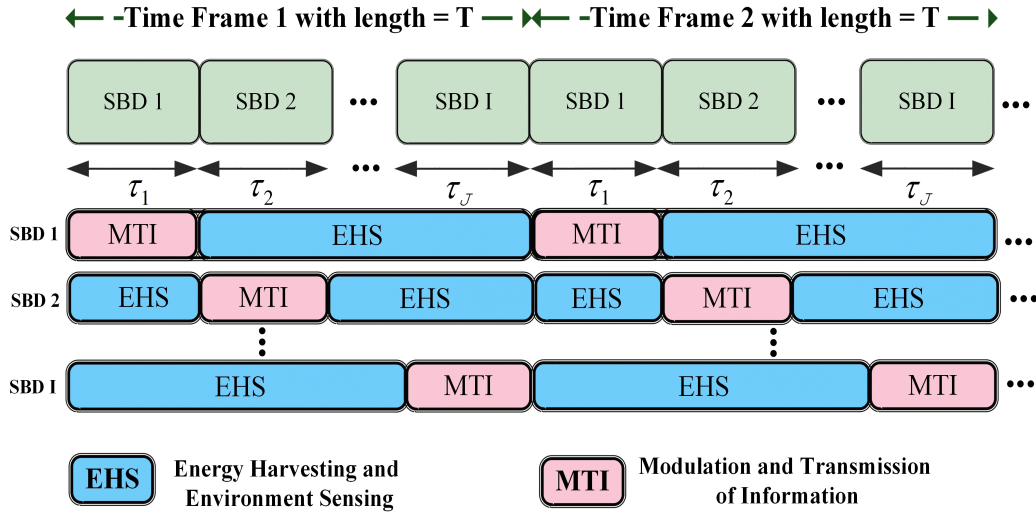
MTI — Modulation and Transmission of Information

Fig. 7: The TDD frame for EHS and MTI modes in TDMA transmission information model

C. Comparison of T-SR and TDMA Modes

After proposing and simulating the SR system to decrease EC in B5G and 6G networks, we intend to compare the scheduling of this system, which was introduced as T-SR with the TDMA scheduling system.

Same as the T-SR mode which was shown in Fig.2, we draw the TDMA mode in Fig.7.

In the TDMA mode, SBDs take turns in transmitting their information in equal time slots in
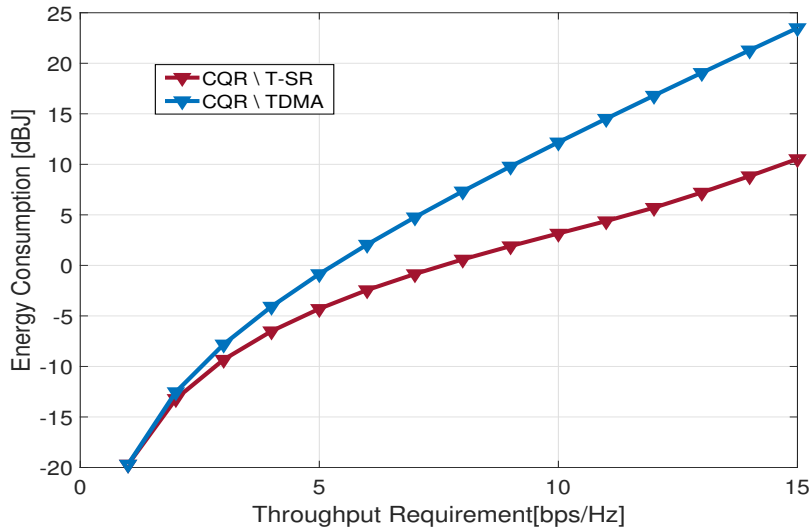
Fig. 8: Comparison of the EC versus SBDs throughput requirement for the T-SR and TDMA scenarios,
$I = 8, N = 9$

time frames [39]. If the amount of information sent in an SBD is large, it is necessary to allocate more slots to those SBDs.

Hereupon, in TDMA mode SBDs may transmit their data discontinuously in more than one-time frame, while in the T-SR mode the transmission data can be completed in one frame and with sequential time slots. The reason is, in TDMA, SBDs only have to send their data in the time slot allocated in that frame.

The T-SR mode is formulated as an SR system, which is the proposed system in this paper. According to the definitions, the TDMA scheme can be considered as a simplified case of T-SR and can be modeled by applying some simplifications to the T-SR model.

In this paper, the TDMA mode is simulated by assuming that it is well implemented in the network and in the receivers no interference occurs. Fig.8 compares the EC of the T-SR mode in the SR network and TDMA mode in typical networks which is presented in Fig.2 and Fig.7, respectively. It is noted that the main purpose of this study is to minimize the amount of energy consumed in the network. According to Fig.8, the EC in the T-SR consumes much less energy than in the TDMA mode (about 8 dB). This is due to the optimal allocation of time slots according to the needs of each SBDs as well as the ability to send information and harvest energy at any time. The difference between the EC of these two systems will increase if the volume of information sent is large and more time slots are needed to send it.

TABLE I: Power Consumption of SR and IoT protocols for one IoT device and in one transmission slot.

IoT Protocols	Frequency Band	Bandwidth	Power Consumption	Reference
SigFox	$902\,MHz$	$200\,KHz$	$\sim 100\,mW$	
LoRa	$928\,MHz$	$500\,KHz$	$\sim 150\,mW$	[2], [61]–[66]
NB-IoT	$1.8\,GHz$	$1\,MHz$	$\sim 500\,mW$	
ZigBee	$2.4\,GHz$	$2\,MHz$	$\sim 100\,mW$	[67], [68]
SR	$2\,GHz$	$400\,KHz$	$\sim 11.6\,mW$	This Paper

D. Comparison Proposed Method With Other IoT Protocols

We know that the use of IoT networks will be very widespread in the future. One of the methods of implementing these networks is to use a semi-passive structure similar to SR system. The SR system is suitable for establishing communications between IoT users and future cellular networks (6G and B5G) and has many advantages such as no need for infrastructure, increased SE and increased EE.

IoT networks can be implemented with other protocols; such as sensor networks that use batteries (e.g., LoRa, ZigBee, ...), or sensors with wirelessly energy harvesting in the wireless powered communication networks (WPCN). In these systems in addition to using active RF energy consuming components such as mixer and power amplifier, a complex electrical and communication infrastructure is required to send information. On the other hand, in the SR system, SBDs use a particular passive structure [27] with the EC being close to zero, as well as the infrastructure of other communication networks such as cellular and Wi-Fi, which greatly reduces energy consumption in the network.

In this section, we intend to compare the EE in a cell with IoT devices that can be implemented with different systems such as SR, ZigBee, LoRa, SigFox and NB-IoT, regardless of the EC of the infrastructure. The EE was defined as the ratio between the instantaneous throughput and the total power consumption in this paper.

The values related to the frequency band, bandwidth and power consumption of each protocol are given in Table I. These values are in accordance with the range specified in their standard. It is also expected that the SR system will be implemented in the approximate range of the frequency band and bandwidth specified in the table (corresponding to ambient waves). The corresponding figure of EE versus SE is drawn in Fig.9. In this simulation, the conditions are considered the same for all systems, and it is assumed that all energy is used for sending and
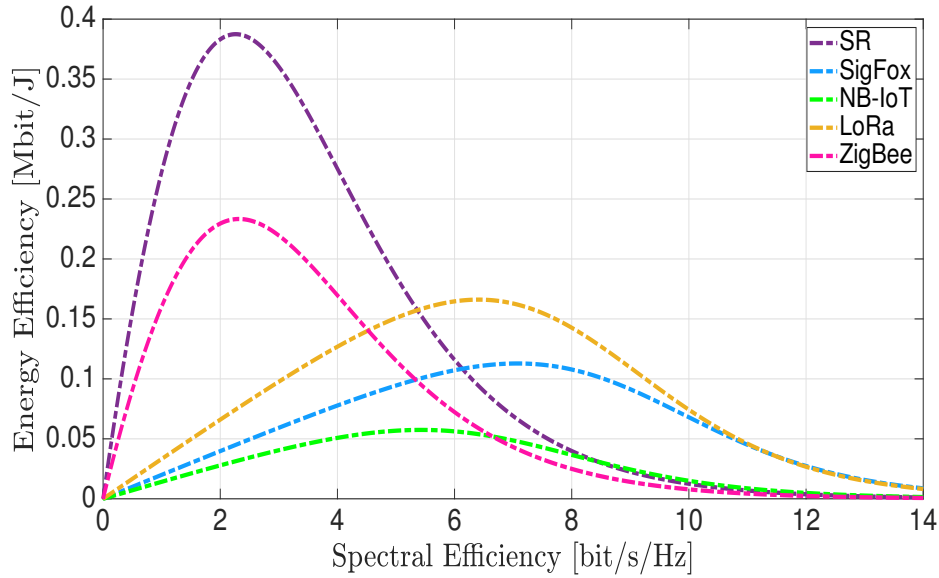
Fig. 9: Energy Efficiency versus Spectral Efficiency between IoT protocols and SR system

receiving information, and no EC is done in the circuit of the device. Furthermore the EC related to the infrastructure of each system is ignored. Also, the diagram is drawn for sending and receiving one signal in a one-time slot.

According to Fig.9, the EE of the SR system is much better than other IoT protocols.

VI. CONCLUSION AND FUTURE WORK

This paper investigated the optimal time and power allocation with novel techniques in the symbiotic radio system for minimizing the EC in a network while satisfying the SBDs throughput requirement. Multiple SBDs harvest energy from ambient signals radiated from BS and then modulate their information on the carrier of that signal and send it to the intended SUE. To achieve the goal of the article, which is to minimize EC in high-density user networks such as B5G and 6G networks, a new technology without special infrastructure and semi-passive called SR has been used. In the SR system, TDMA and timing in SR methods are introduced for scheduling data transmission between SBDs. We formulated the SR system that was a non-convex optimization problem and managed to solve it. The problem becomes a convex and disciplined problem using novel mathematical methods called CQR and SQ. By comparing these two methods, we observed that the CQR method has better EE. Moreover, by changing the basic parameters of the network such as the number of IoT devices and the number of active

massive MIMO antenna in BS, CQR was stable and could further reduce EC in the network. In Fig. 8, we also compared the timing of this proposed system with the TDMA mode (in the SR system), which has a better EE for the reasons explained in the simulation section. Fig.9 presented the power consumption of a network with a large number of IoT users. When they use SR communications, the power consumption of the network is much lower than other current IoT communication protocols. This will have a huge impact to reduce the EC in the future generation networks on a global scale.

There are many ideas for future work, including investigating the spectral efficiency of the proposed system model in this paper, using the intelligence reflect surface (IRS), which is passive structure and will have a great impact on reducing the amount of EC and enhancing spectral and energy efficiency in the network and using the reinforced learning to reduce the EC in the dense IoT networks.

APPENDIX

Lemma: The inequality $g\left(\theta_i, \tau_i\right) \leq g\left(\left(\theta_i, \tau_i\right), \left(\hat{\theta}_i, \hat{\tau}_i\right)\right)$ holds for

$\left(\theta_i, \tau_i\right) \in \left\{\left(\theta_i, \tau_i\right) | \theta_i \geq 0, 0 \leq \frac{\hat{\tau}_i}{\beta} \leq \tau_i \leq \infty\right\}$, where $g\left(\theta_i, \tau_i\right) = \tau_i \log\left(1 + \frac{\theta_i}{\tau_i}\right)$ and $g\left(\left(\theta_i, \tau_i\right), \left(\hat{\theta}_i, \hat{\tau}_i\right)\right)$

is equal to: $\hat{\tau}_i \log\left(1 + \frac{\hat{\theta}_i}{\hat{\tau}_i}\right) + \nabla f\left(\hat{\theta}_i, \hat{\tau}_i\right)\left[\theta_i - \hat{\theta}_i, \tau_i - \hat{\tau}_i\right]^T + \left[\theta_i - \hat{\theta}_i, \tau_i - \hat{\tau}_i\right]\mathbf{H_s}\left[\theta_i - \hat{\theta}_i, \tau_i - \hat{\tau}_i\right]^T$

Proof: We first obtain the minimal matrix $\mathbf{A}$ which satisfies the following relation for $\left(\theta_i, \tau_i\right)$:

$$\mathbf{H_s} = \begin{bmatrix} \frac{\tau_i}{(\tau_i + \theta_i)^2} & -\frac{\theta_i}{(\tau_i + \theta_i)^2} \\ -\frac{\theta_i}{(\tau_i + \theta_i)^2} & \frac{\theta_i^2}{\tau_i(\tau_i + \theta_i)^2} \end{bmatrix} \leq \mathbf{A} = \begin{bmatrix} a_{11} & a_{12} \\ a_{21} & a_{22} \end{bmatrix} \tag{47}$$

According to Eq.(33) the largest value of a_{11} is obtained when θ_i and τ_i have their lowest values

$$a_{11} = \arg\max_{\theta_i, \tau_i}\left\{\tau_i / (\tau_i + \theta_i)^2\right\}\Bigg|_{\substack{\theta_i = 0 \\ \tau_i = \hat{\tau}_i/\beta}} = \beta/\hat{\tau}_i \tag{48}$$

To obtain the maximum value of a_{22} based on the function $\frac{\theta_i^2}{\tau_i(\tau_i + \theta_i)^2}$ is monotonically increasing with respect to θ_i and monotonically decreasing with respect to τ_i:

$$a_{22} = \arg\max_{\theta_i, \tau_i}\left\{\frac{\theta_i^2}{\tau_i(\tau_i + \theta_i)^2}\right\}\Bigg|_{\substack{\text{Lim } \theta_i \to \infty \\ \tau_i = \hat{\tau}_i/\beta}} = \beta/\hat{\tau}_i \tag{49}$$

To obtain $a_{21} = a_{12}$, the derivative of the function $\frac{\theta_i}{(\tau_i + \theta_i)^2}$ is calculated and it is observed that the maximum value of this function is obtained for $\tau_i = \theta_i$ and also τ_i has it's lowest value, so:

$$a_{12} = a_{21} \leq \arg\max_{\theta_i, \tau_i}\left\{\frac{\theta_i}{(\tau_i + \theta_i)^2}\right\}\Bigg|_{\substack{\theta_i = \hat{\tau}_i/\beta \\ \tau_i = \hat{\tau}_i/\beta}} = \beta/4\hat{\tau}_i \tag{50}$$

In addition, to satisfy the above relations, the determinant of the matrix (47) is also greater than zero. By defining an auxiliary variable $\Re$, this inequality will be simplified as follows:

$$\underbrace{\left(a_{11} - \frac{\tau_i}{(\tau_i + \theta_i)^2}\right)}_{\Re_1} \underbrace{\left(a_{22} - \frac{\theta_i^2}{\tau_i(\tau_i + \theta_i)^2}\right)}_{\Re_2} - \underbrace{\left(a_{12} + \frac{\theta_i}{(\tau_i + \theta_i)^2}\right)^2}_{\Re} \geq 0 \tag{51}$$

Consequently, based on Eq.(51) we can calculate the $a_{21} = a_{12}$:

$$a_{12} = a_{21} = -\frac{1}{2}\left(\max\left(\frac{\theta_i}{(\tau_i+\theta_i)^2}\right) - \min\left(\frac{\theta_i}{(\tau_i+\theta_i)^2}\right)\right) = -\frac{1}{2}\left(\frac{\beta}{4\hat{\tau}_i} - 0\right) = -\frac{\beta}{8\hat{\tau}_i} \tag{52}$$

The following inequality is established for $\Re$:

$$\Re \geq \left(-\frac{\beta}{8\hat{\tau}_i} + \frac{\beta}{4\hat{\tau}_i}\right) = \frac{\beta}{8\hat{\tau}_i} \tag{53}$$

and also, we have the following relationships:

$$a_{11} \leq \Re_1 + \frac{\beta}{\hat{\tau}_i} = \frac{9\beta}{8\hat{\tau}_i} \ , a_{22} \leq \Re_2 + \frac{\beta}{\hat{\tau}_i} = \frac{9\beta}{8\hat{\tau}_i} \tag{54}$$

Finally, after these calculations, an upper bound of matrix (32) is shown by Eq.(34).

REFERENCES

[1] Q. Wu, X. Zhou, W. Chen, J. Li, and X. Zhang, "Irs-aided wpcns: A new optimization framework for dynamic irs beamforming," *IEEE Transactions on Wireless Communications*, 2021.

[2] R. K. Singh, P. P. Puluckul, R. Berkvens, and M. Weyn, "Energy consumption analysis of lpwan technologies and lifetime estimation for iot application," *Sensors*, vol. 20, no. 17, p. 4794, 2020.

[3] K. Dev, P. K. R. Maddikunta, T. R. Gadekallu, S. Bhattacharya, P. Hegde, and S. Singh, "Energy optimization for green communication in iot using harris hawks optimization," *IEEE Transactions on Green Communications and Networking*, vol. 6, no. 2, pp. 685–694, 2022.

[4] K. Lee and J. Ko, "Wireless information and power transfer: Probability-based power allocation and splitting with low complexity," *IEEE Systems Journal*, vol. 12, no. 1, pp. 1060–1064, 2016.

[5] R. Oltman, "5g is coming: How t&m manufacturers can prepare for and benefit from 5g," *5G Semiconductor Solutions-Infrastructure and Fixed Wireless Access*, p. 19, 2018.

[6] T. P. Do and Y. H. Kim, "Resource allocation for a full-duplex wireless-powered communication network with imperfect self-interference cancelation," *IEEE Communications Letters*, vol. 20, no. 12, pp. 2482–2485, 2016.

[7] J. Cao, Z. Bu, Y. Wang, H. Yang, J. Jiang, and H.-J. Li, "Detecting prosumer-community groups in smart grids from the multiagent perspective," *IEEE Transactions on Systems, Man, and Cybernetics: Systems*, vol. 49, no. 8, pp. 1652–1664, 2019.

[8] Y. Luo, L. Pu, G. Wang, and Y. Zhao, "Rf energy harvesting wireless communications: Rf environment, device hardware and practical issues," *Sensors*, vol. 19, no. 13, p. 3010, 2019.

[9] S. S. Adhatarao, M. Arumaithurai, D. Kutscher, and X. Fu, "Isi: Integrate sensor networks to internet with icn," *IEEE Internet of Things Journal*, vol. 5, no. 2, pp. 491–499, 2017.

[10] P. Zhang, X. Kang, D. Wu, and R. Wang, "High-accuracy entity state prediction method based on deep belief network toward iot search," *IEEE Wireless Communications Letters*, vol. 8, no. 2, pp. 492–495, 2018.

[11] J. Xie, Z. Chang, X. Guo, and T. Hämäläinen, "Energy efficient resource allocation for wireless powered uav wireless communication system with short packet," *IEEE Transactions on Green Communications and Networking*, 2022.

[12] J. Hu, Q. Wang, and K. Yang, "Energy self-sustainability in full-spectrum 6g," *IEEE Wireless Communications*, vol. 28, no. 1, pp. 104–111, 2020.

[13] D. Niyato, D. I. Kim, M. Maso, and Z. Han, "Wireless powered communication networks: Research directions and technological approaches," *IEEE Wireless Communications*, vol. 24, no. 6, pp. 88–97, 2017.

[14] A. J. Williams, M. F. Torquato, I. M. Cameron, A. A. Fahmy, and J. Sienz, "Survey of energy harvesting technologies for wireless sensor networks," *IEEE Access*, vol. 9, pp. 77 493–77 510, 2021.

[15] T. Sanislav, S. Zeadally, G. D. Mois, and S. C. Folea, "Wireless energy harvesting: Empirical results and practical considerations for internet of things," *Journal of Network and Computer Applications*, vol. 121, pp. 149–158, 2018.

[16] T. Sanislav, G. D. Mois, S. Zeadally, and S. C. Folea, "Energy harvesting techniques for internet of things (iot)," *IEEE Access*, vol. 9, pp. 39 530–39 549, 2021.

[17] N. Su and Q. Zhu, "Power control and channel allocation algorithm for energy harvesting d2d communications," *Algorithms*, vol. 12, no. 5, p. 93, 2019.

[18] D. K. P. Asiedu, S. Mahama, S.-W. Jeon, and K.-J. Lee, "Optimal power splitting for simultaneous wireless information and power transfer in amplify-and-forward multiple-relay systems," *IEEE Access*, vol. 6, pp. 3459–3468, 2018.

[19] V. Liu, A. Parks, V. Talla, S. Gollakota, D. Wetherall, and J. R. Smith, "Ambient backscatter: Wireless communication out of thin air," *ACM SIGCOMM computer communication review*, vol. 43, no. 4, pp. 39–50, 2013.

[20] M. B. Janjua and H. Arslan, "Survey on symbiotic radio: A paradigm shift in spectrum sharing and coexistence," *arXiv preprint arXiv:2111.08948*, 2021.

[21] Z. Chen and B. Ji, "Resource allocation algorithm for iot communication based on ambient backscatter," in *2021 IEEE 93rd Vehicular Technology Conference (VTC2021-Spring)*. IEEE, 2021, pp. 1–5.

[22] L. Zhang, Y.-C. Liang, and M. Xiao, "Spectrum sharing for internet of things: A survey," *IEEE Wireless Communications*, vol. 26, no. 3, pp. 132–139, 2018.

[23] Z. Qin, X. Zhou, L. Zhang, Y. Gao, Y.-C. Liang, and G. Y. Li, "20 years of evolution from cognitive to intelligent communications," *IEEE transactions on cognitive communications and networking*, vol. 6, no. 1, pp. 6–20, 2019.

[24] D. Samanta, C. K. De, and A. Chandra, "Performance analysis of full-duplex multi-relaying energy harvesting scheme in presence of multi-user cognitive radio network," *IEEE Transactions on Green Communications and Networking*, 2022.

[25] Y.-C. Liang, Q. Zhang, E. G. Larsson, and G. Y. Li, "Symbiotic radio: Cognitive backscattering communications for future wireless networks," *IEEE Transactions on Cognitive Communications and Networking*, vol. 6, no. 4, pp. 1242–1255, 2020.

[26] G. Yang, Q. Zhang, and Y.-C. Liang, "Cooperative ambient backscatter communications for green internet-of-things," *IEEE Internet of Things Journal*, vol. 5, no. 2, pp. 1116–1130, 2018.

[27] N. Van Huynh, D. T. Hoang, X. Lu, D. Niyato, P. Wang, and D. I. Kim, "Ambient backscatter communications: A contemporary survey," *IEEE Communications surveys & tutorials*, vol. 20, no. 4, pp. 2889–2922, 2018.

[28] M. N. Mahdi, A. R. Ahmad, Q. S. Qassim, H. Natiq, M. A. Subhi, and M. Mahmoud, "From 5g to 6g technology: meets energy, internet-of-things and machine learning: a survey," *Applied Sciences*, vol. 11, no. 17, p. 8117, 2021.

[29] F. Qamar, M. U. A. Siddiqui, M. N. Hindia, R. Hassan, and Q. N. Nguyen, "Issues, challenges, and research trends in spectrum management: A comprehensive overview and new vision for designing 6g networks," *Electronics*, vol. 9, no. 9, p. 1416, 2020.

[30] C. Huang, S. Hu, G. C. Alexandropoulos, A. Zappone, C. Yuen, R. Zhang, M. Di Renzo, and M. Debbah, "Holographic mimo surfaces for 6g wireless networks: Opportunities, challenges, and trends," *IEEE Wireless Communications*, vol. 27, no. 5, pp. 118–125, 2020.

[31] S. Chen, Y.-C. Liang, S. Sun, S. Kang, W. Cheng, and M. Peng, "Vision, requirements, and technology trend of 6g: How to tackle the challenges of system coverage, capacity, user data-rate and movement speed," *IEEE Wireless Communications*, vol. 27, no. 2, pp. 218–228, 2020.

[32] S. J. Nawaz, S. K. Sharma, B. Mansoor, M. N. Patwary, and N. M. Khan, "Non-coherent and backscatter communications: Enabling ultra-massive connectivity in 6g wireless networks," *IEEE Access*, vol. 9, pp. 38 144–38 186, 2021.

[33] L. Bariah, L. Mohjazi, S. Muhaidat, P. C. Sofotasios, G. K. Kurt, H. Yanikomeroglu, and O. A. Dobre, "A prospective look: Key enabling technologies, applications and open research topics in 6g networks," *IEEE access*, vol. 8, pp. 174 792–174 820, 2020.

[34] A. Patil, S. Iyer, and R. J. Pandya, "A survey of machine learning algorithms for 6g wireless networks," *arXiv preprint arXiv:2203.08429*, 2022.

[35] Z. Dai, R. Li, J. Xu, Y. Zeng, and S. Jin, "Cell-free symbiotic radio: Channel estimation method and achievable rate analysis," in *2021 IEEE/CIC International Conference on Communications in China (ICCC Workshops)*. IEEE, 2021, pp. 25–30.

[36] R. Long, H. Guo, L. Zhang, and Y.-C. Liang, "Full-duplex backscatter communications in symbiotic radio systems," *IEEE Access*, vol. 7, pp. 21 597–21 608, 2019.

[37] R. Long, Y.-C. Liang, H. Guo, G. Yang, and R. Zhang, "Symbiotic radio: A new communication paradigm for passive internet of things," *IEEE Internet of Things Journal*, vol. 7, no. 2, pp. 1350–1363, 2019.

[38] Y. Xu, Z. Qin, G. Gui, H. Gacanin, H. Sari, and F. Adachi, "Energy efficiency maximization in noma enabled backscatter communications with qos guarantee," *IEEE Wireless Communications Letters*, vol. 10, no. 2, pp. 353–357, 2020.

[39] H. Yang, Y. Ye, K. Liang, and X. Chu, "Energy efficiency maximization for symbiotic radio networks with multiple backscatter devices," *IEEE Open Journal of the Communications Society*, vol. 2, pp. 1431–1444, 2021.

[40] Y. Liu, P. Ren, and Q. Du, "Symbiotic communication: Concurrent transmission for multi-users based on backscatter communication," in *2020 International Conference on Wireless Communications and Signal Processing (WCSP)*. IEEE, 2020, pp. 835–839.

[41] S. Han, Y.-C. Liang, and G. Sun, "The design and optimization of random code assisted multi-bd symbiotic radio system," *IEEE Transactions on Wireless Communications*, vol. 20, no. 8, pp. 5159–5170, 2021.

[42] Z. Zhang, Y. Xiao, Z. Ma, M. Xiao, Z. Ding, X. Lei, G. K. Karagiannidis, and P. Fan, "6g wireless networks: Vision, requirements, architecture, and key technologies," *IEEE Vehicular Technology Magazine*, vol. 14, no. 3, pp. 28–41, 2019.

[43] Q. Wu, M. Tao, D. W. K. Ng, W. Chen, and R. Schober, "Energy-efficient resource allocation for wireless powered communication networks," *IEEE Transactions on Wireless Communications*, vol. 15, no. 3, pp. 2312–2327, 2015.

[44] J. Wu, S. Rangan, and H. Zhang, *Green communications: theoretical fundamentals, algorithms, and applications*. CRC press, 2016.

[45] K. Gillingham, R. G. Newell, and K. Palmer, "Energy efficiency economics and policy," National bureau of economic research, Tech. Rep., 2009.

[46] F. Jameel, M. Nabeel, and W. U. Khan, "Multi-tone carrier backscatter communications for massive iot networks," in *Wireless-Powered Backscatter Communications for Internet of Things*. Springer, 2021, pp. 39–50.

[47] Z. Chi, Y. Li, H. Sun, Y. Yao, Z. Lu, and T. Zhu, "B2w2: N-way concurrent communication for iot devices," in *Proceedings of the 14th ACM Conference on Embedded Network Sensor Systems CD-ROM*, 2016, pp. 245–258.

[48] R. Long, Y.-C. Liang, Y. Pei, and E. G. Larsson, "Active-load assisted symbiotic radio system in cognitive radio network," in *2020 IEEE 21st International Workshop on Signal Processing Advances in Wireless Communications (SPAWC)*. IEEE, 2020, pp. 1–5.

[49] M. Asif, A. Ihsan, W. U. Khan, A. Ranjha, S. Zhang, and S. X. Wu, "Energy-efficient backscatter-assisted coded cooperative-noma for b5g wireless communications," *IEEE Transactions on Green Communications and Networking*, 2022.

[50] B. Ling, C. Dong, J. Dai, and J. Lin, "Multiple decision aided successive interference cancellation receiver for noma systems," *IEEE Wireless Communications Letters*, vol. 6, no. 4, pp. 498–501, 2017.

[51] B. R. Marks and G. P. Wright, "A general inner approximation algorithm for nonconvex mathematical programs," *Operations research*, vol. 26, no. 4, pp. 681–683, 1978.

[52] S. Boyd, L. Xiao, and A. Mutapcic, "Subgradient methods," *lecture notes of EE392o, Stanford University, Autumn Quarter*, vol. 2004, pp. 2004–2005, 2003.

[53] Z.-Q. Luo, W.-K. Ma, A. M.-C. So, Y. Ye, and S. Zhang, "Semidefinite relaxation of quadratic optimization problems," *IEEE Signal Processing Magazine*, vol. 27, no. 3, pp. 20–34, 2010.

[54] R. Horst and N. V. Thoai, "Dc programming: overview," *Journal of Optimization Theory and Applications*, vol. 103, no. 1, pp. 1–43, 1999.

[55] J. Nocedal, "Wright st. numerical optimization," 2006.

[56] J. F. Sturm, "Using sedumi 1.02, a matlab toolbox for optimization over symmetric cones," *Optimization methods and software*, vol. 11, no. 1-4, pp. 625–653, 1999.

[57] S. Boyd, S. P. Boyd, and L. Vandenberghe, *Convex optimization*. Cambridge university press, 2004.

[58] A. Ben-Tal and A. Nemirovski, "On polyhedral approximations of the second-order cone," *Mathematics of Operations Research*, vol. 26, no. 2, pp. 193–205, 2001.

[59] Y. Ye, *Interior point algorithms: theory and analysis*. John Wiley & Sons, 2011.

[60] A. Ben-Tal and A. Nemirovski, *Lectures on modern convex optimization: analysis, algorithms, and engineering applications*. SIAM, 2001.

[61] B. Martinez, M. Monton, I. Vilajosana, and J. D. Prades, "The power of models: Modeling power consumption for iot devices," *IEEE Sensors Journal*, vol. 15, no. 10, pp. 5777–5789, 2015.

[62] M. S. Mahmoud and A. A. Mohamad, "A study of efficient power consumption wireless communication techniques/modules for internet of things (iot) applications," 2016.

[63] J. Finnegan and S. Brown, "An analysis of the energy consumption of lpwa-based iot devices," in *2018 International Symposium on Networks, Computers and Communications (ISNCC)*. IEEE, 2018, pp. 1–6.

[64] D. Poluektov, M. Polovov, P. Kharin, M. Stusek, K. Zeman, P. Masek, I. Gudkova, J. Hosek, and K. Samouylov, "On the performance of lorawan in smart city: End-device design and communication coverage," in *International Conference on Distributed Computer and Communication Networks*. Springer, 2019, pp. 15–29.

[65] M. Lauridsen, R. Krigslund, M. Rohr, and G. Madueno, "An empirical nb-iot power consumption model for battery lifetime estimation," in *2018 IEEE 87th Vehicular Technology Conference (VTC Spring)*. IEEE, 2018, pp. 1–5.

[66] E. Bäumker, A. M. Garcia, and P. Woias, "Minimizing power consumption of lora® and lorawan for low-power wireless sensor nodes," in *Journal of Physics: Conference Series*, vol. 1407, no. 1. IOP Publishing, 2019, p. 012092.

[67] S. K. Gharghan, R. Nordin, and M. Ismail, "Energy-efficient zigbee-based wireless sensor network for track bicycle performance monitoring," *Sensors*, vol. 14, no. 8, pp. 15573–15592, 2014.

[68] O. O. Kazeem, O. O. Akintade, and L. O. Kehinde, "Comparative study of communication interfaces for sensors and actuators in the cloud of internet of things," *Int. J. Internet Things*, vol. 6, no. 1, pp. 9–13, 2017.